MF4.2 (Contributed)
4:00 PM - 4:15 PM

Continuous control of microring weight banks

A. N. Tait, M. A. Nahmias, T. Ferreira de Lima, B. J. Shastri,
A. X. Wu, E. Zhou, E. C. Blow, and P. R. Prucnal
Princeton University, Princeton, NJ, 08544 USA
atait@princeton.edu

***Abstract*—We demonstrate a continuous range of complementary (+/–) weights in a bank of silicon microrings. Continuously configurable weighted addition is a key function for multivariate analog signal processing and could enable scalable analog networking approaches in silicon photonics.**

The rapid development of CMOS-compatible photonic interconnect technologies has inadvertently opened a door for unconventional circuit and system opportunities in optics. At the same time, microelectronic fields have recently renewed investigation of non-von Neumann architectures, in part, due to incipient limitations in aspects of Moore's law. In what is considered the 3rd generation of "neuromorphic" architectures, most approaches incorporate time-resolved dynamics, loosely classified as "spiking," in addition to decentralizing processing – a move that intimately intertwines interconnection with computing. Photonics device research has followed suit with a recent bloom of proposed forms of spiking dynamics [1]; however, few suitable optical interconnects have been proposed. In the past, neural networking ideas implemented in holograms have failed to outperform mainstream electronics at relevant problems in computing, which can largely be attributed to their incompatibility with mainstream integration technologies.

A recent proposal for wavelength-division multiplexed (WDM) networks based on microring resonator (MRR) weight banks could endow a potential photonic neural network with compatibility with silicon photonic platforms [2]. Weighted addition is a generic type of analog fan-in, which describes how signals from multiple sources (e.g. multiple sensors, or other nodes in a network) are combined. The WDM version of weighted addition is a critical subcircuit for constructing potential all-analog, all-optical networks in an integrated photonic substrate (Fig. 1).

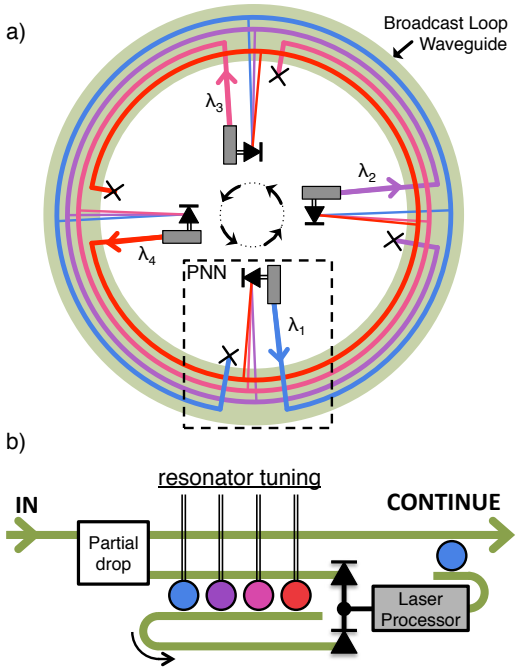

Fig. 1. a) Concept of a broadcast-and-weight network, from [2]. WDM signals are transported between processing-networking nodes (PNNs) by a loop waveguide. b) A PNN circuit. Signals on the bus are partially dropped, then a tunable filter bank independently routes channel power between opposing ports of a balanced photodetector. Continuous weight bank tuning enables effective weights from –1 to +1. Photodetectors act simultaneously as transducers and additive computational elements, solving both challenges of physical fan-in and efficient λ-conversion.

Prior work demonstrating a parallel MRR filter bank for weighting WDM signals showed that effective signal polarity (+/–) could be switched using a balanced photodetector (PD) [3]. The ability to change weight polarity, in addition to magnitude, is essential for analog processing and networking based on weighted addition; however, analog magnitude control was not shown. Due to the extreme sensitivity of high-Q MRR features to fabrication and environmental factors, thermal control has been explored extensively in the context of WDM demultiplexers and modulators [4]. Commonly, the goal of MRR control is to track a particular point in the resonance relative to the signal carrier wavelength, such as the center or maximum slope point.

In this work, we demonstrate MRR weight control over the continuous range of weights from –1 to +1, and show that a feedforward calibration approach is sufficient to do so. Although several MRR control approaches are based on feedback, the unique topology of a MRR weight bank, in which multiple filtered channels remain multiplexed until detection, makes it more difficult to monitor the complete state of the bank; however, in-ring power monitoring devices could be applicable [4].

Silicon-on-insulator samples were fabricated through UBC SiEPIC; silicon thickness is 220nm with fully etched waveguides. Fibers are coupled to chip using focusing subwavelength grating couplers [5]. Ti/Au tuning contacts were then deposited on top of an oxide passivation layer. The device consists of two bus waveguides and four 6-8μm radius MRRs in a parallel

978-1-4799-7465-8/15/$31.00 ©2015 IEEE

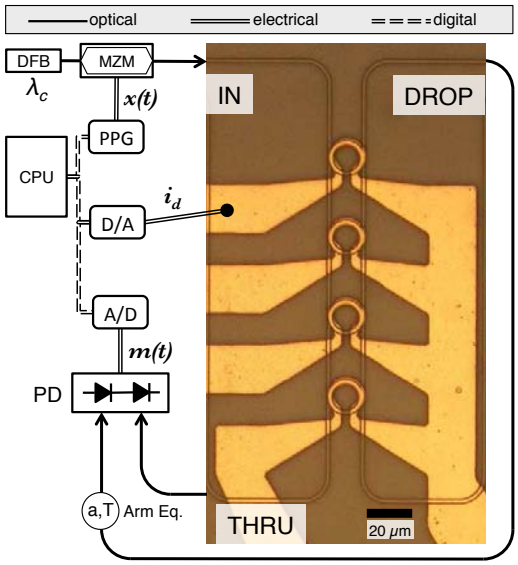

Fig. 2. Experimental setup, including optical micrograph of the 4-filter weight bank, wherein all filters drop into the same waveguide. A tuning current i_d is applied to heat one MRR filter (common sink connection not shown). The input consists of a 2Gbps PRBS signal, $x(t)$, modulated on an optical carrier at λ_c =1551.668nm. The DROP and THRU outputs of the filter bank, after fixed amplitude and delay equalization, are sent to opposing ports of a balanced photodiode (PD), yielding the weighted signal, $m(t)$. Instruments (PPG, D/A converter, and A/D converter) are controlled on a digital communication bus, which allows the CPU to estimate the effective weight value and perform automated weight calibration. Not shown: tunable laser source and optical spectrum analyzer configured to monitor device transmission.

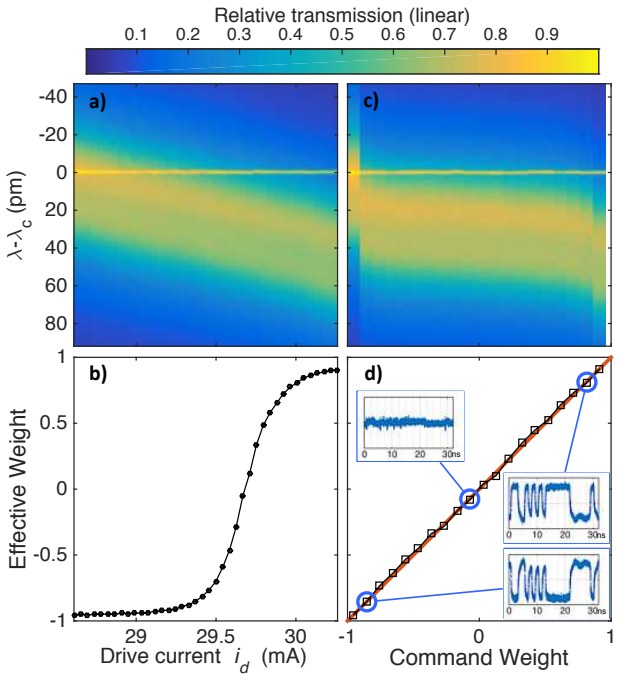

Fig. 3. (a-b) Initial sweep in drive current: a) shows filter relative transmission spectra vs. drive current. The input signal, which is stronger than the spectrum analyzer's swept laser source, is visible at $\lambda - \lambda_c = 0$. b) Measured weight vs. drive current, showing a full range from -1 to 1 attained with balanced detection. Weight values are calculated using the correlation between input and output signals, Eq. (1). This curve is used as an estimate of the tuning function, $\hat{f}$. (c-d) Calibrated sweep in command weight: c) the shift in filter resonant wavelength is a strongly nonlinear function of the command weight, which roughly reflects the inverse of the tuning function estimate from (b), such that in d) there is a well-controlled, direct correspondence between command and effective weight. The ideal x=y line is plotted in red. Insets show output signal traces at positive, negative, and zero effective weights.

add/drop configuration, each with a thermal tuning element (Fig. 2). The sample is mounted on a temperature-controlled alignment stage. The experimental setup consists of computer-controlled instruments for generating optical signals, applying current to the sample, and measuring the resultant weighted output. A digital pulse pattern generator (PPG) is used for convenience, although signals are treated as analog.

Calibration is performed in two stages once the tuning region of interest is manually identified (in this case, 29-30 mA). First, the tuning current is swept in order to estimate the tuning function, f, that maps drive current, i_d, to effective weight, μ.

$$\mu \equiv \langle x(t) \cdot m(t) \rangle_t = f(i_d) \tag{1}$$

where $\langle \cdot \rangle_t$ is a time average. Once f is estimated, it's inverse is computed to yield a calibration rule:

$$i_d = \hat{f}^{-1}(\hat{\mu}) \tag{2}$$

where $\hat{f}$ is the estimated tuning function and $\hat{\mu}$ is the command weight. Because of the sharp nonlinearity of f, its initial estimate is poorly sampled, leading to an inaccurate calibration. The calibration is refined by performing a sweep in $\hat{\mu}$ and updating the estimate of $\hat{f}$, the result of which is shown in Fig. 3d. The results indicate that simple resonance tuning with feedforward calibration is sufficient to reliably attain a continuous range of analog weight values, even despite the sensitivity of this regime.

Further directions would include controlling multiple MRRs within a single bank. Because of the sensitivity of the resonance, cross-talk (thermal, optical, and amplifier gain saturation) must be accounted for, which could increase the challenge of simple calibration based on function inversion. An investigation of how the weight impacts dispersive effects on analog signal integrity is also important for increasing bandwidth performance. Continuous control of a single MRR weight is a key step towards the goal of multivariate analog signal processing in a silicon photonic platform.

References

[1] M. A. Nahmias *et al.*, *J. Selected Topics in Quantum Elec.*, vol. 19, no. 5, 2013.

[2] A. N. Tait *et al.*, *J. Lightwave Technol.*, vol. 32, no. 21, pp. 3427–3439, Nov 2014.

[3] A. Tait *et al.*, in *Summer Topicals, 2015 IEEE/OSA*, July 2015.

[4] S. Grillanda *et al.*, *Optica*, vol. 1, no. 3, pp. 129–136, Sep 2014.

[5] Y. Wang *et al.*, *Optics express*, vol. 22, no. 17, pp. 20 652–20 662, 2014.